

SEISMIC IMAGING OF THE CENTRAL TAUPO VOLCANIC ZONE USING DOUBLE-DIFFERENCE TOMOGRAPHY

Stephen Bannister¹, Sandra Bourguignon¹, Steve Sherburn² and Ted Bertrand²

¹GNS Science, 1 Fairway Drive, Avalon, Lower Hutt 5010, New Zealand

² GNS Science, Wairakei, New Zealand

s.bannister@gns.cri.nz

Keywords: *Passive seismology, seismic tomography, Taupo Volcanic Zone, earthquake, seismic properties.*

ABSTRACT

We image the crustal seismic properties beneath a 30x50 km area encompassing the Wairakei, Mokai, Rotokawa, Ngatamariki, and Ohaaki geothermal fields, as part of a multi-disciplinary research program to investigate the untapped deep geothermal resource north of Taupo. A broadband seismometer array comprised of 38 seismometer sites was deployed across the region between 2009 and 2011, recording more than 500 earthquakes. We use the travel-times of these earthquakes to derive 3D P-wave and S-wave velocity structure, using double-difference seismic tomography. The derived 3-D Vp and Vp/Vs volumes highlight a high level of spatial and depth heterogeneity of the seismic properties beneath the study region, and provide new information on large-scale structures that may influence the deep geothermal resources. This study of seismic properties is complementary to magnetotelluric studies by GNS Science investigating electrical conductivity in the same region (e.g. Bertrand et al., 2012). The relocated seismicity provides the best dataset to date of earthquake locations in the TVZ; we observe areas where the inferred brittle-ductile transition appears to be several kms deeper than the previously assumed 6-8 km.

1. INTRODUCTION

1.1 Background

The Taupo Volcanic Zone (TVZ) is an actively rifting continental arc (Wilson et al., 1995) that is related to subduction of the Pacific Plate beneath the North Island of New Zealand, along the Hikurangi margin. The central part of the TVZ, north of Lake Taupo (Figure 1), is marked by extensive rhyolitic volcanism and includes 23 high-temperature geothermal systems. Development of 'conventional' geothermal energy, from depths of 1-3 km where reservoir temperatures reach 330°C contributes ~13% (~800 MWe) of New Zealand's electricity supply. However, estimates of the deep geothermal resources at depths of up to 5-7 km (where temperatures are likely to exceed 400°C) could exceed 10,000 MWe (Bignall, 2010).

To better understand New Zealand's deep geothermal resource potential, a research programme was established in 2008 to investigate links between the shallow hydrothermal systems and the deeper magmatic heat source that is thought to drive convection within the brittle crust. This research included the collection of Magnetotelluric (MT) and passive-seismic measurements in the southeast part of the TVZ. These complementary MT and passive-seismic surveys aim to identify structure within the basement rocks at depths between 3 and 8 km that advance our understanding of the process that transport heat to the surface. Research to date has included very intensive magnetotelluric observations and

3D inversion for electrical properties of the mid-crust (Bertrand et al., 2012; Heise et al., 2010).

In the seismic investigation, outlined here, we invert data from a 'deep geothermal' passive-seismic array, in order to define the variation of the bulk seismic properties of the crust in the same region as already covered by the magnetotelluric observations, focusing especially on the 3-to-8 km depth range. We do this using double-difference seismic tomography (Zhang and Thurber, 2003; 2006; Zhang et al., 2009).

The seismic properties we target include P-wave velocity (Vp), the S-wave velocity (Vs), and the Vp/Vs ratio, while in later studies we will also invert the seismic waveform characteristics for 3D variation of seismic attenuation (1/Qp and 1/Qs), which is an excellent indicator of temperature. As an additional side-product of the inversion studies the data provide the opportunity to examine the spatial variation in earthquake depths across the region, which inform us on spatial changes in the brittle-ductile transition associated with temperature.

1.2 Seismic Data

We utilise seismic data recorded using a dense 38-site broadband seismic array which was deployed across the region between September 2009 and April 2011, with an average station spacing of ~4-6 km. The array seismometer locations are shown in Figure 1.

We supplement this new broadband data with legacy short-period and broadband data recorded by previous research seismic arrays, collected from 1995 onwards, including the 1995 "TVZ95" array (Bryan et al., 1999; Sherburn et al., 2003), the 2001 "CNPSE" array (Reyners et al., 2006), broadband array data collected in 2004, short-period and broadband data recorded by the national GeoNet seismometer network (Petersen et al., 2011), and active- (explosion) source data collected in the "NIGHT"-experiment in 2001 (Harrison and White, 2006; Henrys et al., 2003) (Figure 1). The combined dataset is comprised of 1198 well-recorded earthquakes (Figure 3) and 9 explosions, recorded at 925 recording stations, providing more than 120,000 differential travel time measurements, which were calculated using the absolute times from pairs of neighbouring earthquakes. We hand-picked P-phase and S-phase arrival times for all of the earthquakes recorded by the 2009-2011 broadband seismic array, subsequently assigning arrival-pick uncertainties automatically on the basis of the signal-to-noise ratio. P-arrival times were picked on vertical component data, and S-wave arrivals were picked on horizontal component data, where available, out to stations more than 120 km offset from the epicenter. Previous seismic data and seismic arrival time phase picks from previous seismic experiments were re-examined manually before incorporating into the full combined dataset. Additional S-phase arrival times were picked for many of the legacy datasets.

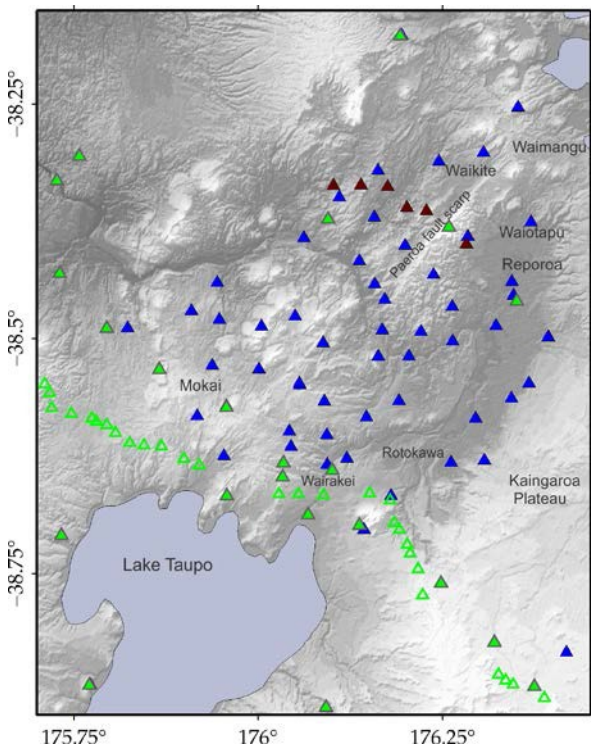


Figure 1: Distribution of seismometers deployed in the Taupo Volcanic Zone, for which seismic data were available for this study. Station symbols are CNIPSE: green solid triangles; Harrison & White array: green open-triangles; HD2009-2011 array: blue triangles; RF2004 array: red triangles. The earlier TVZ95 array (1995) is not shown.

2. INVERSION FOR VELOCITY STRUCTURE

Given the available seismological data, we then retrieve and iterate on the velocity model, to examine the velocity heterogeneity and variations in travel-path travel times away from the earthquake source.

2.1 Approach

Here we apply the double-difference (DD) tomography method ‘tomoDD’ of Zhang and Thurber (2003) to jointly invert for earthquake hypocentres, and seismic parameters P- wave velocity (V_p), S-wave velocity (V_s) and V_p/V_s . The technique of Zhang and Thurber minimizes residuals between observed and calculated arrival-time differences for pairs of closely located earthquakes, while also minimizing the residuals of absolute arrival times. This approach builds on the DD location procedure of Waldhauser and Ellsworth (2000), which utilises the differential times of catalog P and S phase times. In addition to solving for the hypocentral parameters, the tomoDD algorithm solves for the 3-D velocity structure in the model region, requiring an additional smoothing parameter and damping parameter, as described by Zhang and Thurber (2003). In this initial analysis described here we only utilise catalog differential times, which are derived from the phase pick arrival times of the P and S phases. The use of differential arrival-time data, in addition to catalog absolute-time data, can improve the absolute location of earthquakes, as well as the relative locations of

earthquakes within clusters (Menke and Schaff, 2004). Compared to absolute travel times, differential travel times are less sensitive to near-surface heterogeneity and variations in travel-path away from the earthquake source. Absolute earthquake locations derived from double difference inversion (Waldhauser, 2001; Waldhauser & Ellsworth, 2000), as carried out here, have a much better accuracy than usually recognised (Menke and Schaff, 2004).

In future anticipated work we plan to carry out refined analysis on our hypocentre relocations, which will also involve the calculation and use of waveform-based differential times from the earthquake waveform data, in order to provide further constraint on the earthquake depths. Accurate absolute earthquake depths are critical for further interpretation, as they will constrain the lateral variation of the brittle-ductile transition beneath the region, which varies as a function of the crustal temperature.

Initial hypocenter locations for the double-difference inversion were those determined by GeoNet, for events detected and located by GeoNet, although some additional events were also included which weren't originally located by GeoNet. The full range of earthquakes in the combined inversion dataset comprises an excellent range of shallow crustal earthquakes, located from Lake Taupo up to Tarawera, as well as deeper background seismicity, comprised of larger earthquakes occurring in the subducted Pacific plate, which lies at greater than 50 km depth beneath the TVZ region. The information contained in the arrival-times from the deeper subduction earthquakes (which range between 40 and 200 km depth) helps to constrain the deeper crustal structure, while the shallower earthquakes provide the detailed information for refining the shallow crustal structure. The final data set provides the best possible coverage of the shallow Taupo Volcanic Zone (TVZ) crustal structure to date, of any seismic data set, and, apart from Kawerau, samples beneath most of the geothermal fields currently tapped for geothermal power. New additional GeoNet stations are installed in the region each year. In the future we will use data from any additional stations to further improve the raypath coverage through the upper-mid crust, and further improve the resolution of the seismic property volumes derived from that data.

Catalog-based differential times (CTDT) were calculated between closely spaced events from manually picked P- and S- phase times. Differential times were calculated for event pairs initially separated by less than 10 km, for all stations less than 140 km from the particular cluster centroid. Use of such a maximum separation criteria reduces the total number of required correlation calculations, but is justifiable, as the correlation between different events typically decreases rapidly with increasing inter-event separation, and the assumptions underlying the use of differential times also becomes poor with increasing event separation (Waldhauser, 2001; Waldhauser & Ellsworth, 2000). Once calculated, the CTDT differential times were then combined with the absolute arrival times (arrival times of picked P and S phases) and simultaneously inverted using tomoDD (Zhang and Thurber, 2003) in an iterative least-squares procedure which utilises the LSQR method (Paige and Saunders, 1982). The full dataset was comprised of 25820 absolute P-times, 13596 absolute S phases, 13141 absolute S-P times, and 128559 differential times.

The initial velocity model used for travel-time calculations was a modified version of the New Zealand 3D velocity model, derived by Eberhart-Phillips et al., (2010) from earthquake data. The 3D New Zealand model is quite well defined in the Taupo Volcanic Zone, down to more than 300 km depth, primarily as a result of intensive tomography work carried out in 2001-2006 (Eberhart-Phillips et al, 2010; Reyners et al, 2006), where passive-source seismic data from the North Island CNIPSE experiment (Reyners et al., 2006) was used to constrain the model. However the density of seismometer stations during the 2001 CNIPSE experiment was not adequate to provide high resolution of shallow-mid crustal properties (which is one reason why this current study is necessary).

For this study we gradationally interpolated the 3D New Zealand model velocities onto a much finer grid to encompass our study region. Our final finest-level inversion grid has a minimum grid spacing of 7.5 km along the x- and y-axes, in the section of the inversion volume with the highest ray path coverage, and grid layers at 1, 2.5, 4, 5.5, 7, 9, 11, 14, 18, 23, 30, 34, and 38 km depth, in the top 40 kms, fully encompassing the range of depths of interest (Figure 2). Deeper inversion nodes were retained from the New Zealand 3D wide velocity grid, down to depths of 367 km. Our inversion strategy involved slowly increasing the inversion node density, starting with the New Zealand wide 3D velocity grid, and slowly increasing the node density between inversions, to the grid density described above. This gradational approach to the velocity inversion has been recognised in other studies to provide stable results, especially critical for heterogeneous regions such as the TVZ.

The 3D V_p , V_s and V_p/V_s velocity structure was then modified as part of the tomographic inversion. In addition the 1198 earthquakes used in the inversion were relocated using the final 3D V_p and V_p/V_s solution models and the P and S cross-correlation times optional to the double-difference method (Waldauser, 2001). Additional work in the future will further refine the earthquake locations, using waveform differential times.

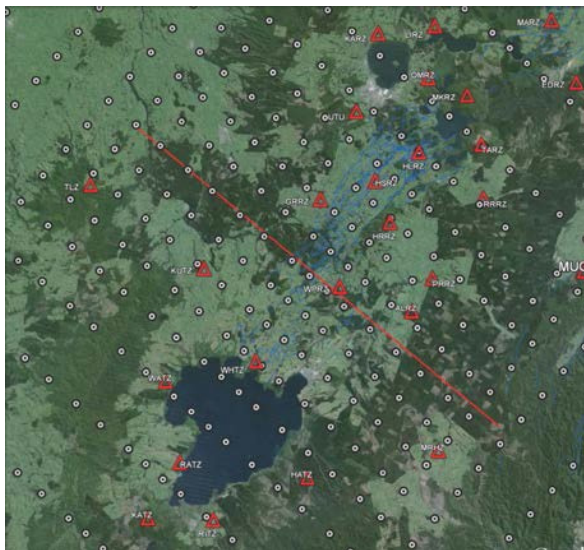


Figure 2: Location of the inversion nodes are shown as white circles. The location of the cross-section used for Figure 7 is marked as a red line. GeoNet seismometer stations are shown as red triangles.

Figure 4 shows depth slices of the resulting P-wave velocity (V_p) volume after inversion, sliced horizontally at 4 and 6 km depth below sea level. We use the derivative weight sum (DWS) (Thurber, 1993) at each grid node as a measure of the raypath coverage and resolution. The velocity structure is well resolved in the centre of the study region (inside the bounds of the 2009-2011 seismometer array), although not to the east, on the Kaingaroa Plateau, nor west of Lake Atiamuri, due to the lack of recording seismometer stations to the west and north-west, and the lower level of seismicity activity at crustal depths on the areas west and east of the TVZ.

3. SEISMIC PROPERTIES AND SEISMICITY

Figure 4 shows the P-wave velocity at 4 and 6 kms depth, as well as the relocated seismicity projected onto each depth slice. At 4 kms depth we note seismic activity (projected from 4 +/- 1km) associated with west Wairakei geothermal field and Rotokawa geothermal field, as well as north of Waiotapu, while at 6 (+/- 1 km) depth there is seismicity north-west of Waimungu, and also near Mokai. Further relocation analysis using waveform-based differential travel times (e.g. Walhauser, 2001, Waldhauser & Ellsworth, 2000, Zhang and Thurber, 2006) is necessary to confirm the depth of the seismic-aseismic transition, and whether there are substantial spatial changes in the transition depth beneath the region, and beneath individual geothermal fields. Any such changes that we determine are expected to closely relate to spatial changes in the temperature. Low V_p , less than 5 km/s, is observed at 4 km depth in the area north-west of Waikite, and also along the north edge of Lake Taupo. At 6 km depth (Figure 4) V_p varies between ca.5.3 km/s and 6 km/s, with lower V_p values west of the Paeroa fault scarp.

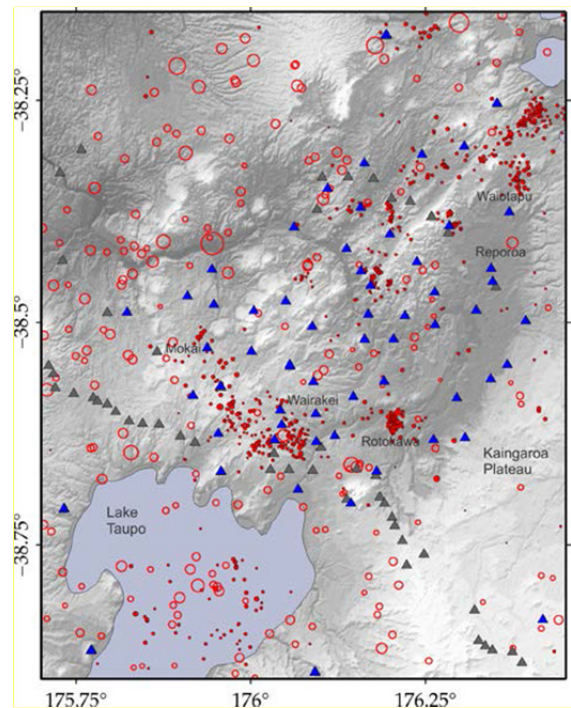


Figure 3: Distribution of 1198 earthquakes used in the tomographic inversion. Solid red circles represent events shallower than 40 km; open red circles are earthquakes deeper than 40 km. Blue triangles are the 2009-2011 broadband array, grey triangles are all other seismometer sites, inclusive of GeoNet.

Figure 5 shows the S-wave velocity also at 4 and 6 kms depth. At 6 km depth we note Vs values slightly higher than 3 km/s, with Vs around 3.5-3.6 km/s beneath Wairakei geothermal field. Such a velocity may relate to the presence of a plutonic body at that depth, but confirmation of such an interpretation really requires detailed seismic attenuation studies, which are currently in process – the dense waveform database we now have is ideal for detailed 3D attenuation inversion work. Cross-parameter examination (e.g. direct comparison between Vp, Vs, and Vp/Vs, attenuation, and resistivity values) will also be used for further interpretation, following work by Zhang et al (2009) and Bedrosian et al (2007).

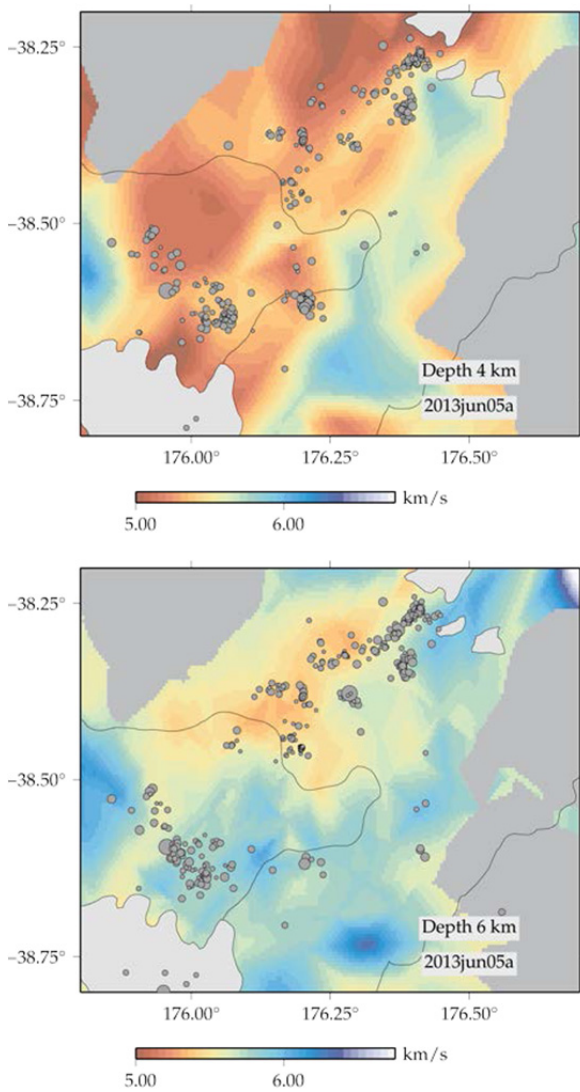


Figure 4: P-wave velocity (km/s) at (top) 4 km depth and (bottom) 6 km depth. At 4 km depth we note the seismic activity associated with west-Wairakei geothermal field, Rotokawa geothermal field, and the area near north of Waiotapu. At 6 km seismic activity is observed north-west of Waimangu, Earthquakes within +/- 1 km of each depth slice are projected onto the slice. A grey mask is applied for areas with DWS (P-wave Derivative weight sum) less than 100.

Figure 6 shows the Vp/Vs ratio at 4 and 8 kms depth. The comparison between the spatial variation of Vp/Vs at the two depths illustrates the high level of 3D heterogeneity within the crust beneath the region ; the two depth slices are only 2 km apart, yet Vp/Vs clearly changes rapidly with depth. Seismicity west of Wairakei geothermal field, at 8 +/- 1 km depth, appears to relate to a low Vp/Vs area. Low Vp/Vs, less than 1.65, is observed beneath Ngatamariki field at 6 km depth.

A quartz-rich granitoid composition would be expected to result in low Vp/Vs and Poissons ratio (Christensen, 1996). If this interpretation is correct, then the Vp/Vs image suggests that, just north of Lake Taupo, the transition in the terranes is actually just west of Wairakei. This possible interpretation is complicated however by the possibility that Vp/Vs in this region can be influenced by the presence of remnants of volcanic intrusion (e.g. Husen et al, 2012). Again, the variability of the derived Vp/Vs, both spatially and in depth, highlights that simplistic 2-D models of the TVZ crust are inappropriate.

Figure 7 shows cross-sections of the derived Vp and Vp/Vs, slicing through the volumes at a strike of N120E, following the cross-section shown in Figure 2. The cross-section of Vp shows a fairly high level of 3D heterogeneity, especially at ca 5-15 kms depth, while there are also large-scale (> 20% variability over 20 km) changes in Vp at 10-30 kms depth, especially moving between Lake Taupo and north- Reporoa (profile not shown). It is clear that simplistic 2-D interpretations of TVZ crustal structure are not appropriate for the central TVZ. At the shorter scale, slices of the Vp volume suggest small, thin, higher Vp bodies at between 5 and 10 km depth. These may possibly represent solidified plutonic material (e.g. Wilson et al.,2006). The scale of these bodies appears to be around 5 km, which is certainly around the resolution limit of our data inversion. Further resolution testing and synthetic modelling needs to be carried out to confirm the details of the bodies.

Vp/Vs (shown in Figure 6; Figure 7) shows a marked change between the south-east and the north-west, with lower Vp/Vs values at ca. 5-to-15 km depth compared to the western end of the profile. Given that low Vp/Vs is observed well beneath the Kaingaroa plateau, the change in Vp/Vs may be reflecting the changing nature of the basement terrane, from the Torlesse (composite) Terrane to the east, dominated by quartz-rich turbidites, and of plutoniclastic granitoid composition , to the Waipapa Terrane to the west, which is increasingly felsic (Adams et al., 2009; Mortimer et al, 1997).

If this interpretation is correct, then the Vp/Vs image suggests that, just north of Lake Taupo, the transition in the terranes is actually just west of Wairakei. This possible interpretation is complicated however by the possibility that Vp/Vs in this region can be influenced by the presence of remnants of volcanic intrusion. Again, the variability of the derived Vp/Vs, both laterally and in depth, highlights that simplistic 2-D models of the TVZ crust are inappropriate.

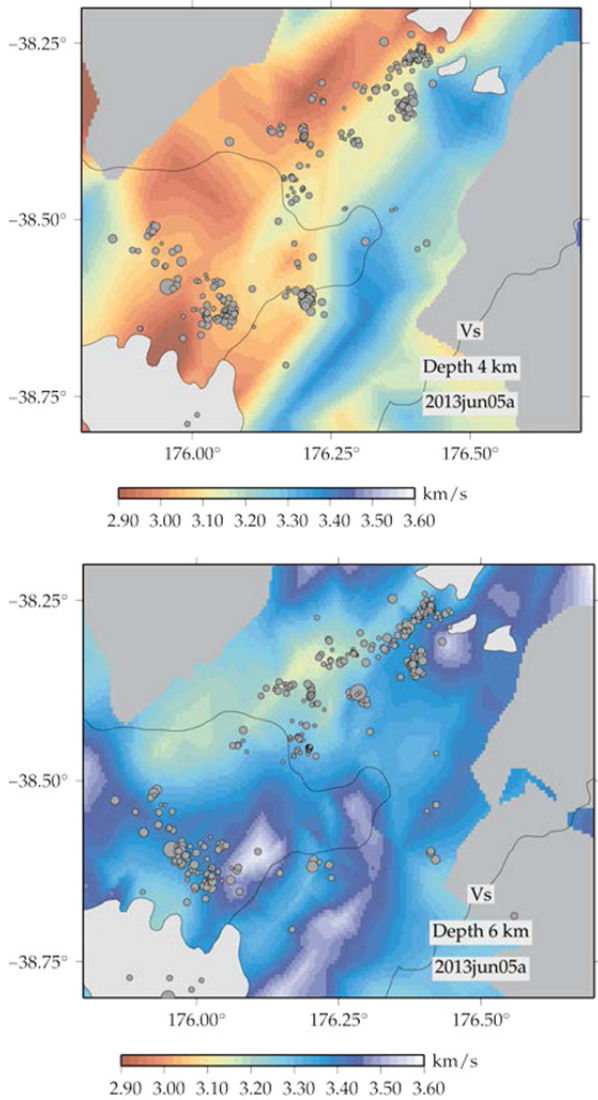


Figure 5: S-wave velocity (km/s) at: (top) 4 km depth and (bottom) 6 km depth. At 6-km depth we note Vs slightly higher than 3.4 km/s beneath Wairakei geothermal field, and higher Vs extending north from Lake Taupo, towards Rotokawa geothermal field. Areas that are not well constrained are masked.

2. CONCLUSION

We investigate seismic properties (Vp, Vs, Vp/Vs) in the mid-crust of the central Taupo Volcanic Zone, focusing on the 3-to-8 km depth range. Intensive passive-seismic array measurements were carried out by GNS Science between 2009 and 2011, using a 38-station broadband and short-period seismometer array, to improve resolution of existing velocity models in the region north of Lake Taupo and south of Reporoa caldera. Analysis of the new passive seismic data, wrapped in together with existing passive-source and active-(explosion) source data that were collected in previous seismological investigations, highlights the high variability of the seismic properties in 3D, at a variety of scales. Further detailed analysis will focus on defining the 3D variation of seismic attenuation properties, using the full seismic wavefield, and also on defining the lateral and depth variation of the seismic-aseismic transition beneath the region.

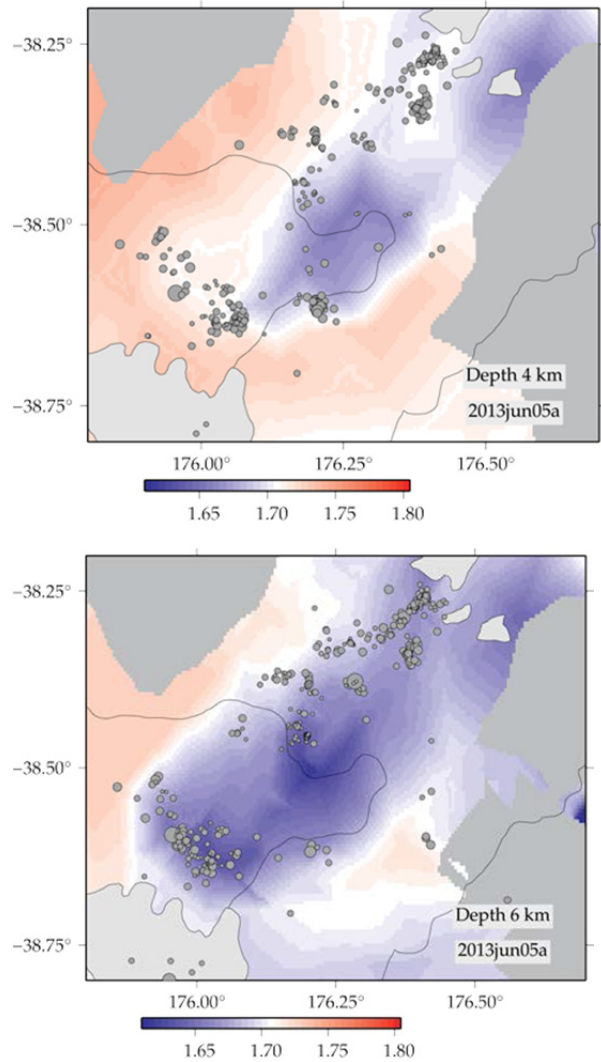


Figure 6: Vp/Vs ratio at (top) 4 km depth and (bottom) 6 km depth. Seismicity at 6 km (+/- 1km) west of Wairakei geothermal field appears to lie within an area with low Vp/Vs (< 1.68). Areas that are not well constrained are masked.

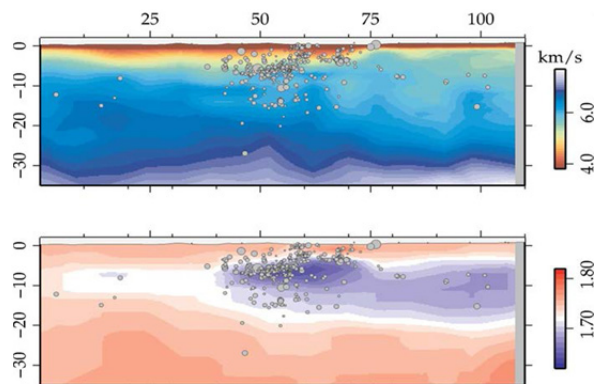


Figure 7: Vp (top) and Vp/Vs (bottom) along a cross-section across the Taupo Volcanic Zone, along the cross-section marked in Figure 2. Note the large lateral change in Vp/Vs at 5-to-15 km depth. Depth-axis is in kms, X-axis distance is in kms.

ACKNOWLEDGEMENTS

We thank Craig Miller, Nick Horspool, GNS Science Wairakei technicians, and GNS Science Wairakei staff for their logistical support in the seismic data collection during 2009-2011. National seismometer network data were provided by GeoNet, which is sponsored by the New Zealand Government through its agencies: Earthquake Commission (EQC), GNS Science, and Land Information New Zealand (LINZ). We used GMT (Wessel & Smith, 1998) and Obspy (Beyreuther et al, 2010) for figures. This research was carried out under the GNS Science CORE geothermal programme, funded by the New Zealand government.

REFERENCES

Adams, C.J. Mortimer, N., Campbell, H.J., Griffin, W.L., 2009. Age and isotopic characterisation of metasedimentary rocks from the Torlesse Supergroup ad Waipapa Group in the central North Island, New Zealand, *New Zealand Journal of Geology and Geophysics*, 52:2, 149-170.

Bedrosian, P.A., Maercklin,N., Weckmann, U., Bartov, Y., Ryberg, T., ad O.Ritter, (2007). Lithology-derived structure classification from the joint interpretation of magnetotelluric and seismic models. *Geophys. J. Int.*, 170(2), 737-748.

Bertrand, T., Caldwell, T.G et al., 2012. Deep geothermal exploration in the Taupo Volcanic Zone with an array of magnetotelluric and passive-seismic data. *New Zealand Geothermal Workshop Proceedings*, 2012.

Beyreuther, M., Barsch, R., Krischer, L., Megies, T., Behr, Y., and J.Wassermann, (2010). ObsPy: A python toolbox for seismology, *Seismological Research Letters*, doi:10.1785/gssrl.81.3.530.

Bignall, G., Hotter and Deeper: New Zealand's research programme to harness its deep geothermal resources. *Proceedings World Geothermal Congress*, 2010, Bali, Indonesia, 25-29 April 2010.

Bryan, C.J., Sherburn, S., Bibby, H.M., Bannister, S., Hurst, A.W., 1999. Shallow seismicity of the central Volcanic Zone, New Zealand : its distribution and nature. *New Zealand Journal of Geology and Geophysics*, 42(4): 533-542.

Christensen, N.I. (1996). Poissons ration and crustal seismology. *J.Geophys.Res.*, 101, p319-3156.

Eberhart-Phillips, D., Reyners, M.E., Bannister, S., Chadwick, M.P., Ellis, S.M., 2010. Establishing a versatile 3-D seismic velocity model for New Zealand. *Seismological research letters*, 81(6):992-1000. doi: 10.1785/gssrl.81.6.992.

Harrison, A.J., and R.S.White (2006). Lithospheric structure of an active backarc basin: the Taupo Volcanic Zone, New Zealand. *Geophysical Journal International*, 167, 969-990, doi:10.1111/j.1365-246X.2006.03166.x

Heise, W., Caldwell, T.G., Bibby, H.M., and S.L.Bennie, 2010. Three-dimensional electrical resistivity image of magma beneath an active continental rift, Taupo Volcanic Zone, New Zealand. *Geophysical Research Letters*, 37, L10301, doi:10.1029/2010GL043110.

Henrys, S., Bannister, S., Pecher, I.A., Davey, F.J., Stern, T., Stratford, W., White, R., Harrison, A.J., Nishimura, Y., Yamada, A., 2003. New Zealand North Island GeopHysical Transect (NIGHT): field acquisition report. Lower Hutt: Institute of Geological & Nuclear Sciences Limited. *Institute of Geological & Nuclear Sciences science report 2003/19*. 49 p.

Menke, W., and D. Schaff (2004). Absolute earthquake locations with differential data. *Bull. Seism.Soc.Am.*, 94, 2254-2264.

Paige, C., and M., Saunders (1982). LSQR: An algorithm for sparse linear equations and least squares problems, *Trans. Math. Software*, 8, 43-71.

Petersen, T., Gledhill, K., Chadwick, M., Gale, N.H., and J.Ristau (2011). The New Zealand national seismograph network. *Seismological research letters*, 81, doi: 10.1785/gssrl.82.1.9

Reyners, M.E., Eberhart-Phillips, D., Stuart, G., Nishimuria, Y., 2006. Imaging subduction from the trench to 300 km depth beneath the central North Island, New Zealand, with Vp and Vp/Vs. *Geophysical Journal International* 165(2): 565-583.

Sherburn, S., Bannister, S., Bibby, H.M., 2003. Seismic velocity structure of the central Volcanic Zone, New Zealand, from local earthquake tomography. *Journal of Volcanology and Geothermal Research*, 122(1-2): 69-88.

Thurber, C.H. (1993). Local earthquake tomography: Velocities and Vp/Vs – Theory, in *Seismic Tomography: Theory and Practice*, edited by H.Iyer and K.Hirahara, pp. 563-580, CRC Press, Boca Raton, Fla.

Waldhauser, F., and W.L. Ellsworth (2000). A double-difference earthquake location algorithm,: Method and applicaton to the northerm Hayward fault, California. *Bull.Seismological Society Am.*, 90, 1353-1368.

Waldhauser, F., (2001). hypoDD – A program to compute double-difference hypocenter locations (hypoDD version 1.0-03/2001). *USGS Open File report 01-11*.

Wessel, P., and W.H.F. Smith (1998). New, improved, version of the Generic Mapping Tools released, *EOS Trans.AGU*, 79, 579, 1998.

Wilson, C.B., Blake, S., Charlier, B>L.A., and A.N.Sutton, (2006). The 26.5 kz Oruanui Eruption, Taupo Volcano, New Zealand: Development, characteristics and evacuation of a large rhyolitic magma body, *Journal of Petrology*, 47, 35-69.

Zhang, Haijiang, & Thurber, C. (2006). Development and Applications of Double-difference Seismic Tomography. *Pure and Applied Geophysics*, 163(2-3), 373–403. doi:10.1007/s00024-005-0021-y

Zhang, Haijiang, Thurber, C., & Bedrosian, P. (2009). Joint inversion for Vp, Vs, and Vp/Vs at SAFOD, Parkfield, California. *Geochemistry Geophysics Geosystems*, 10(11), 1-17. doi:10.1029/2009GC002709

Zhang, Haijiang, & Thurber, C. H. (2003). Double-Difference Tomography: The Method and Its Application to the Hayward Fault, California. *Bulletin of the Seismological Society of America*, 93(5), 1875–1889. doi:10.1785/0120020190